Dalton
Transactions

RSCPublishing

PAPER

View Article Online
View Journal | View Issue

Cite this: *Dalton Trans.*, 2013, **42**, 14545

Novel mixed-valence Cu compounds formed by Cu^{II} dimers with double oximato bridges: *in situ* formation of anionic layer $[Cu_2(SCN)_3]_n^{n-}$†

Piu Dhal,[a] Madhusudan Nandy,[a] Dipali Sadhukhan,[a] Ennio Zangrando,[b] Guillaume Pilet,[c] Carlos J. Gómez-García[d] and Samiran Mitra*[a]

Received 13th June 2013,
Accepted 22nd July 2013

DOI: 10.1039/c3dt51561c

www.rsc.org/dalton

Two new N_3O donor ketoxime Schiff bases (HL^1 and HL^2) have been synthesized by condensing *N*,*N*-dimethylethylenediamine with diacetylmonoxime and benzilmonoxime, respectively in a 1 : 1 ratio. Reaction of $Cu(ClO_4)_2·6H_2O$ with HL^1 resulted in a discrete oximato-bridged dinuclear Cu^{II} complex $[Cu_2(L^1)_2(H_2O)_2](ClO_4)_2$ (**1**). The same reaction in presence of NaSCN affords the complex $\{[Cu^{II}_2(L^1)_2]-[Cu^{I}_4(\mu_{1,3}\text{-SCN})_4(\mu_{1,1,3}\text{-SCN})_2]\}_n$ (**2**), where partial $Cu^{II}\rightarrow Cu^{I}$ reduction is observed. In **2**, arrays of $[Cu^{II}_2(L^1)_2]^{2+}$ cationic units are inserted in between 2D $\{[Cu^{I}_4(SCN)_6]^{2-}\}_n$ layers and connected *via* $\mu_{1,1,3}$-SCN^- links, thus forming a 3D network. On the other hand, reaction of $Cu(CH_3COO)_2$ and HL^2 in the presence of NaSCN gave rise to a mixed-valence pentanuclear cluster $\{[Cu^{II}_2(L^2)_2(NCS)]_2[Cu^{I}(SCN)(\mu_{1,1}\text{-SCN})(\mu_{1,3}\text{-SCN})]\}$ (**3**) where Cu^{II} is also partly reduced to Cu^{I}. In compound **3**, two cationic $[Cu^{II}_2(L^2)_2(NCS)]^+$ units are bridged by the anionic $[Cu^{I}(SCN)_3]^{2-}$ unit through long Cu–SCN linkages. The ligands and the complexes have been characterized by elemental analysis, UV/Vis and IR spectroscopy. The complexes are further characterized by single crystal X-ray diffraction and variable temperature magnetic (VTM) studies. Finally a complete magneto-structural correlation has been established between compounds **1–3** and all the characterized Cu dimers with a double NO bridge.

Introduction

The chemistry of polynuclear mixed-valence $Cu^{I,II}$ complexes has drawn current interest with the aim to elucidate the activities of various multi-copper blue oxidase enzymes such as laccase and ascorbate oxidase.[1,2] In addition they have found applications in catalysis[3] and molecular magnetism.[4] Mixed-valence copper complexes are of special interest because copper(II) and copper(I) prefer different geometries and stereochemistries and both oxidation states are highly labile and stereochemically flexible,[5,6] which is not usually the case for mixed-valence Fe, Co and Ru compounds. These $Cu^{I,II}$ complexes can largely be grouped into four classes[7] containing (i) Cu^{II} cations and Cu^{I} anions or *vice versa*,[8] (ii) Cu^{II} and Cu^{I} centers bridged by polydentate ligands,[9] (iii) Cu^{II} and Cu^{I} centers bridged by CN^-/SCN^-/$SeCN^-$ pseudohalides,[10] and finally (iv) complexes with Cu^{II} and Cu^{I} centers enclosed in a cluster.[11] Partial reduction of Cu^{II} to Cu^{I} in polynuclear copper(II) complexes has been observed to take place in the presence of SCN^- or CN^-.[12]

The study of polynuclear complexes of transition metals with pseudo-halide bridges is also intriguing from a structural point of view because of the different modes of coordination to the metal ions.[13] The linear pseudohalide SCN^- with three different atoms linearly disposed can coordinate metal ions in both terminal and bridging modes. In bi- and poly-nuclear systems different coordination modes of SCN^- have been identified, namely *cis*-$\mu_{1,3}$-NCS (A),[14] $\mu_{1,1}$-NCS (B),[15] $\mu_{1,1}$-SCN (C),[16] $\mu_{1,1,3}$-SCN (D)[17] and $\mu_{1,1,1,3}$-SCN (E)[18] (Scheme 1). Modes A, C and D are observed in the present study.

Our interest in the coordination chemistry of oximato-bridged copper complexes stems from both structural and magnetic points of view.[19–23] Ligands containing oximate groups (=N–O⁻) are able to generate di-, oligo- and poly-nuclear complexes as they have versatile bridging units to bind metal ions through the oximato nitrogen and oxygen atoms in

---

[a] Department of Chemistry, Jadavpur University, Raja S. C. Mullick Road, Kolkata 700032, West Bengal, India. E-mail: samiranju92@gmail.com; Fax: (+91) 33 2414 6414; Tel: (+91) 33 2414 6666 x2779

[b] Department of Chemical and Pharmaceutical Sciences, Via Licio Giorgieri 1, 34127 Trieste, Italy

[c] Université de Lyon, Université Claude Bernard Lyon 1, Laboratoire des Multimatériaux et Interfaces (LMI), UMR 5615 CNRS-UCBL, Groupe de Cristallographie et Ingénierie Moléculaire, Bât. Chevreul, 43 Bd du 11 Novembre, 1918, 69622 Villeurbanne Cedex, France

[d] Instituto de Ciencia Molecular (ICMol), Universidad de Valencia, Catedrático José Beltrán, 2, 46980 Paterna, Spain

† Electronic supplementary information (ESI) available: Additional figures. Packing diagram of the complex **1** (Fig. S1), packing diagram of the complex **3** (Fig. S2). CCDC 929096–929098 (for **1**, **2** and **3** respectively). For ESI and crystallographic data in CIF or other electronic format see DOI: 10.1039/c3dt51561c

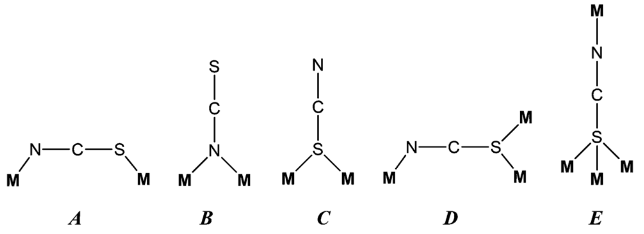

Scheme 1 Different coordination modes of the thiocyanate ligand.

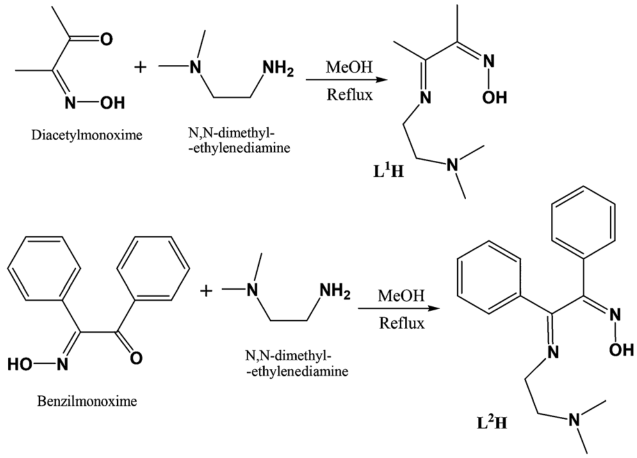

Scheme 2 The synthetic routes of the Schiff base ligands.

three different ways.[24–29] A cooperative –NO– bridged dinuclear cluster usually contains a central six-membered (–Cu–N–O–)$_2$ ring that, if planar, leads to strongly antiferromagnetically coupled Cu$^{\text{II}}$ ions, while a weak antiferromagnetic or ferromagnetic behavior is observed in the case of a non-planar conformation.[30,31]

In this paper we report three oximato-bridged copper complexes with two related ketoxime Schiff-bases (HL^1 and HL^2) obtained by condensing diacetylmonoxime and benzilmonoxime with *N*,*N*-dimethylethylenediamine in a 1 : 1 molar ratio (Scheme 2). The reaction of copper perchlorate with HL^1 leads to the formation of a discrete dinuclear complex [Cu$_2$(L^1)$_2$(H$_2$O)$_2$] (ClO$_4$)$_2$ (**1**). On the other hand, the reaction carried out in the presence of SCN$^-$ leads to *in situ* Cu$^{\text{II}}$→Cu$^{\text{I}}$ partial reduction generating a mixed-valence 3D network $\{[\text{Cu}^{\text{II}}{}_2(\text{L}^1)_2][\text{Cu}^{\text{I}}{}_4(\mu_{1,3}\text{-SCN})_4(\mu_{1,1,3}\text{-SCN})_2]\}_n$ (**2**) with HL^1, and a mixed-valence pentanuclear cluster $\{[\text{Cu}^{\text{II}}{}_2(\text{L}^2)_2(\text{NCS})]_2[\text{Cu}^{\text{I}}(\text{SCN})(\mu_{1,1}\text{-SCN})(\mu_{1,3}\text{-SCN})]\}$ (**3**) with HL^2. This metal reduction is a usual phenomenon when Cu$^{\text{II}}$ salts are subjected to solvothermal conditions in the presence of SCN$^-$ ligand,[9] but here CuSCN-based coordination polymers were obtained starting from a Cu$^{\text{II}}$ salt under non-hydrothermal reaction conditions. In accordance with previously reported planar oximato-bridged copper Schiff base compounds, likewise complexes **1**, **2** and **3** show strong antiferromagnetic interactions.[32]

Results and discussions

Crystal structure of [Cu$_2$(L^1)$_2$(H$_2$O)$_2$](ClO$_4$)$_2$ (1)

A perspective view of the complex cation of **1** is shown in Fig. 1 and the main bond lengths and angles are listed in Table 1.

The complex consists of a dinuclear copper core with the metals connected by the oximato oxygen of the chelating ligands. Both copper centers present a square pyramidal geometry with the basal plane formed by the oximato, the imine and the free amine nitrogen donors of one chelating (L^1)$^-$ ligand and by the oximato oxygen of the other and *vice versa*. A water molecule completes the coordination environment of each metal ion at the apical position. The Cu–OH$_2$ bond distances, of 2.450(12) and 2.407(8) Å, are significantly longer than the equatorial Cu–O ones of 1.882(4), 2.004(4) Å for Cu1 and Cu2, respectively. These apical water molecules form an intramolecular hydrogen bond with a distance of 2.993(14) Å. With the aqua ligands being on the same side with respect to the (CuL^1)$_2$ mean plane, the complex possesses an

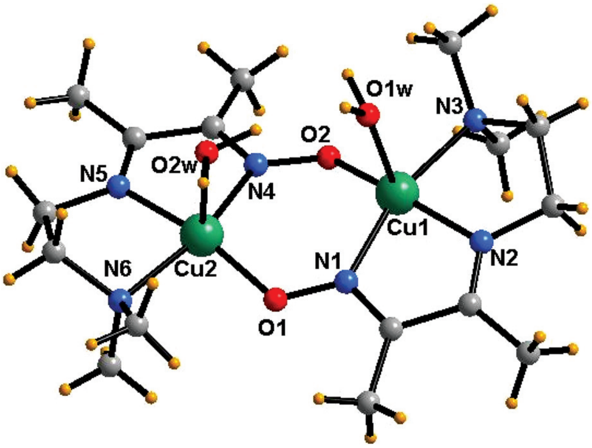

Fig. 1 Perspective view of the complex cation of **1**.

Table 1 Selected bond lengths (Å) and angles (°) for complex **1**

Bond lengths			
Cu1–O2	1.883(4)	Cu2–O1	1.888(3)
Cu1–N1	2.009(4)	Cu2–N4	2.003(4)
Cu1–N2	1.930(5)	Cu2–N5	1.934(4)
Cu1–N3	2.053(4)	Cu2–N6	2.059(4)
Cu1–O11	2.414(9)	Cu2–O21	2.393(8)
Bond angles			
O2–Cu1–N1	103.47(16)	O1–Cu2–N4	104.31(14)
O2–Cu1–N2	162.31(19)	O1–Cu2–N5	168.26(17)
O2–Cu1–N3	90.50(18)	O1–Cu2–N6	90.52(16)
N1–Cu1–N2	80.53(16)	N4–Cu2–N5	80.45(16)
N1–Cu1–N3	163.77(17)	N4–Cu2–N6	162.77(17)
N2–Cu1–N3	83.69(18)	N5–Cu2–N6	83.38(18)
O11–Cu1–O2	99.2(3)	O21–Cu2–N4	93.6(2)
O11–Cu1–N1	93.2(2)	O21–Cu2–N5	96.0(2)
O11–Cu1–N2	97.7(3)	O21–Cu2–N6	94.0(2)
O11–Cu1–N3	92.7(2)	O21–Cu2–O1	94.4(2)

approximate C_2 symmetry. The trigonality τ index is 0.026 for Cu1 and 0.100 for Cu2 ($\tau = |\beta - \alpha|/60°$ where β and α are the two largest angles around the metal atom; $\tau = 0$ for a perfect square pyramidal geometry, and $\tau = 1$ for a regular trigonal bipyramidal geometry).[33] Cu1 and Cu2 atoms are displaced from the basal N_3O donor plane towards the apical water molecule by 0.198 and 0.149 Å, respectively. The metals are separated by 3.623(1) Å, which is within the range of the reported distance separation in $\mu_{1,2}$-N,O double oximato-bridged Cu_2 complexes.[32,34]

The crystal packing (Fig. S1†) shows one perchlorate located in channels outlined by the metal complexes down axis-*b*, the other occupying the metal axial positions, with a $O_3ClO\cdots Cu$ distance of *ca.* 3.62 Å. Dinuclear molecules are alternately packed with parallel and perpendicular orientations with respect to each other along the *bc* plane. The nearest inter-dimer Cu1···Cu2 distance between two parallel-stacked molecules is 7.692 Å whereas it is 7.015 Å between two perpendicularly-stacked molecules.

Crystal structure of $\{[Cu^{II}_2(L^1)_2][Cu^{I}_4(\mu_{1,3}\text{-SCN})_4(\mu_{1,1,3}\text{-SCN})_2]\}_n$ (2)

The asymmetric unit of **2** consists of half the reported formula, being the dinuclear complex cation located on a crystallographic inversion center (Fig. 2). A selection of bond lengths and angles is reported in Table 2. The structure of the dinuclear cation $[Cu^{II}_2(L^1)_2]^{2+}$ is comparable to that of **1**, except for the axial water molecules that are now replaced by SCN^- ligands located on different sides of the basal planes. The metal atoms in **2** are separated by 3.650(1) Å. The square pyramidal coordination geometry ($\tau = 0.078$) of the Cu^{II} ions is formed by the chelating tridentate N donors of the Schiff base and the oximato oxygen O1 of the symmetry-related ligand. The Cu–O and Cu–N bond lengths are comparable to those observed in complex **1**. The apical position is occupied by a semi-coordinated sulfur atom (S2) of the $\mu_{1,1,3}$-SCN^- ligand from the anionic part with a rather long Cu1–S2 bond distance of 2.875(3) Å.

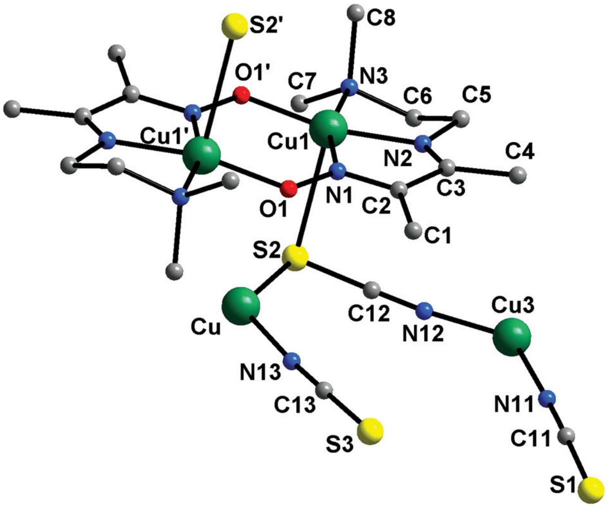

Fig. 2 View of the dinuclear Cu^{II} complex (located on an inversion center) and of the asymmetric unit of the anionic moiety of **2** (primed atoms at $-x$, $-y + 1$, $-z + 1$).

Table 2 Selected bond lengths (Å) and angles (°) for complex **2**[a]

Bond lengths			
Cu1–O1	1.879(8)	Cu2–N13	1.900(10)
Cu1–N1	1.995(9)	Cu2–S2	2.252(3)
Cu1–N2	1.921(10)	Cu2–S3^i	2.208(3)
Cu1–N3	2.090(9)	Cu3–N11	1.890(11)
Cu1–S2	2.875(3)	Cu3–N12	1.865(11)
		Cu3–S1^{ii}	2.287(3)
Bond angles			
S2–Cu1–O1	95.6(2)	N1–Cu1–N3	163.1(4)
S2–Cu1–N1	87.7(2)	N2–Cu1–N3	83.0(4)
S2–Cu1–N2	95.4(2)	S2–Cu2–N13	117.1(3)
S2–Cu1–N3	95.0(2)	S2–Cu2–S3^i	120.36(13)
O1–Cu1–N1	105.7(4)	S3^i–Cu2–N13	122.3(3)
O1–Cu1–N2	167.8(3)	N11–Cu3–N12	130.2(5)
O1–Cu1–N3	90.8(3)	S1^{ii}–Cu3–N11	113.6(4)
N1–Cu1–N2	80.1(5)	S1^{ii}–Cu3–N12	116.1(4)

[a] Symmetry codes: (i) $-x, y - 1/2, -z + 3/2$; (ii) $-x + 1, y - 1/2, -z + 3/2$.

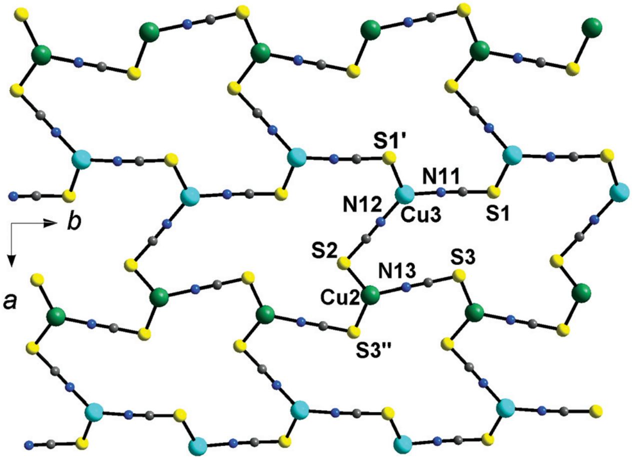

Fig. 3 $[Cu^I\text{-}SCN]_n$ layer of (6,3) topology in compound **2** developed parallel to the crystallographic *ab* plane.

The most interesting feature of the crystal packing of **2** is the formation of 2D anionic layers formulated as $[Cu^I_2(SCN)_3]_n^{n-}$, constructed by two independent copper(I) ions with a trigonal planar coordination, and by three SCN^- anions. The (6,3) net topology, having almost coplanar atoms, is depicted in Fig. 3 and comprises 24-membered metallacycles. The independent atoms Cu2 and Cu3 have S_2N and N_2S chromophores, respectively, connected by two thiocyanate ligands with a $\mu_{1,3}$-SCN^- bridging mode, while the third SCN^- ligand presents a $\mu_{1,1,3}$-SCN^- coordination mode. Here the Cu^I–S and Cu^I–N distances vary in the range 2.208(3)–2.286(3) Å, and 1.864(11)–1.900(10) Å, respectively. As can be seen in Fig. 3 the SCN coordination through nitrogen is practically linear (C–N–Cu^I bond angles are between 174.5(11) and

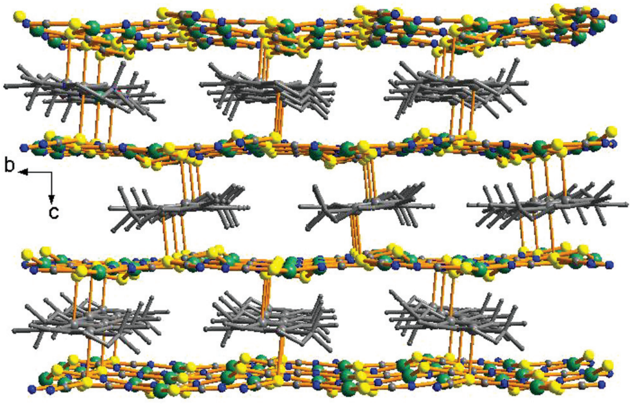

Fig. 4 Perspective view of the Crystal packing showing the Cu complexes sandwiched by the [Cu–SCN]$_n$ layers.

177.6(11)°), while the C–S–Cu^I values fall within 99.5(4) and 104.1(4)°.

Thus the $\mu_{1,1,3}$-SCN$^-$ ligand through the bridging S2 atom is connected to the divalent metal Cu1 of the cationic unit, the Cu(2)–S(2)–Cu(1) bridging angle being 103.23(12)°. As a result, a 3D architecture is formed where the dinuclear complexes are sandwiched in between the anionic layers, a perspective view of which is shown in Fig. 4.

Crystal structure of {[Cu$^{II}{}_2$(L^2)$_2$(NCS)]$_2$[Cu^I(SCN)($\mu_{1,1}$-SCN)($\mu_{1,3}$-SCN)]} (3)

The X-ray structural analysis of **3** revealed that this compound is a pentanuclear complex containing five crystallographically independent Cu ions (Fig. 5). The complex can be best described as formed by two dinuclear cationic entities (A and A′) connected to a central anionic fragment [Cu^I(SCN)$_3$]$^{2-}$ (B) (Fig. 5).

Both dinuclear entities A and A′ present a similar conformation and the bond distances and angles (Table 3) are similar to those measured in **1** and **2**, indicating a clear tendency of these ligands to form similar dinuclear species, having in each case a double NO-bridged cationic dinuclear core. The basal plane of all the Cu^{II} atoms in the dinuclear fragments is formed in a similar way to that observed in complexes **1** and **2**. In each case a SCN$^-$ ligand completes the square pyramidal coordination geometry at the axial position. However, the metals Cu2 and Cu5 are connected to a terminal thiocyanate ligand *via* a nitrogen donor (with a mean Cu–N bond length of 2.163(8) Å), while Cu1 and Cu4 are connected through the S atom to a $\mu_{1,3}$-SCN$^-$ and a $\mu_{1,1}$-SCN$^-$ ligand of entity B (Cu–S = 2.608(3) and 2.709(3) Å, respectively). The trigonality τ index values are comparable and very close to zero (range 0.022–0.062).[33] In **3** the Cu1⋯Cu2 and Cu4⋯Cu5 separations are 3.653(1) and 3.642(1) Å, similar to the distance found in complex **2**. The central entity B is composed of a Cu^I atom (Cu3) bound to three SCN$^-$ ligands, each showing a different connectivity (Fig. 6). In fact, the trigonal coordination plane around Cu3 is composed of the sulfur S2 from a terminal SCN$^-$, S3 from a $\mu_{1,1}$-bridging SCN$^-$, and of nitrogen N15 from a $\mu_{1,3}$-bridging SCN$^-$, the latter two connecting copper ions of entities A′ and A, as described above. The NCS anions are arranged about Cu3 with a geometry similar to that observed in **2** for Cu2: the connection *via* the N atom is almost linear (171.0(10)°), while the connections through the S atoms present Cu3–S–C bond angles of 103.3(6) and 104.9(4)°. The shorter Cu^I–Cu^{II} distance inside the complex is 3.771(1) Å (Cu3⋯Cu4, through the bridging sulfur S3 of Fig. 6).

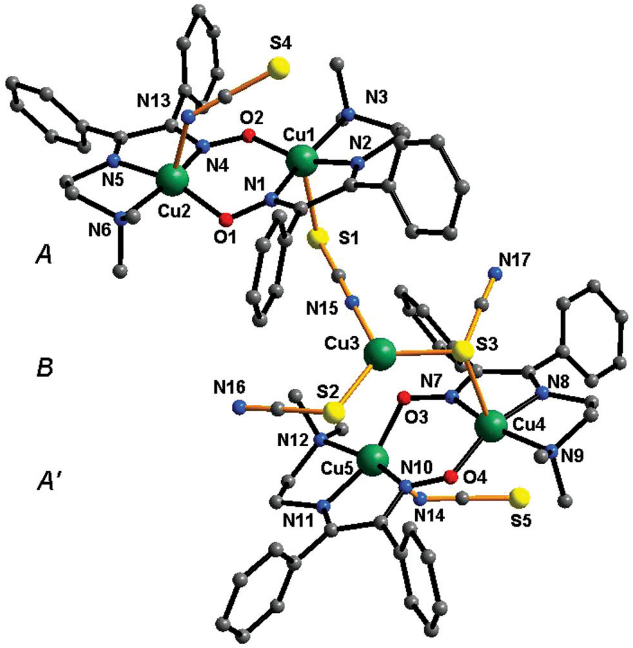

Fig. 5 View of the pentanuclear cluster of complex **3** with indication of the A, A′ and B entities, For clarity H atoms are omitted and only non-C atoms are labeled.

The presence of the Cu^I–(SCN)$_3$ moiety with the thiocyanate ligands acting with different coordination modes towards two divalent dinuclear complexes represents a very unique feature of compounds **2** and **3**. In fact, a search in the CCDC database shows that **3** is the first Cu/SCN complex with such a connectivity as displayed in Fig. 6.

The crystal packing (Fig. S2†) does not show any particular feature, and there are no π–π interactions among the phenyl rings. The pentanuclear molecules are packed in a parallel fashion along the *ac* plane where the nearest Cu^{II}⋯Cu^{II} distance 9.964 Å is observed between Cu2 and Cu4 along the *b* axis and 13.039 Å between Cu2 and Cu5 along the *a* axis.

The differences between **2** and **3** can be explained from the different sizes of the substituent groups in the ligands. In fact, the dinuclear Cu^{II} units in **3** are bulkier than those of complex **2**, since the methyl groups of L^1 have been replaced by phenyl groups in L^2. The lesser steric hindrance of complex **2** allows the accommodation of dinuclear cationic moieties in between the 2D anionic layers, leading to a 3D network, whereas in complex **3**, probably due to the steric hindrance of the bulky phenyl rings, only two discrete dinuclear units are associated

Table 3 Selected bond lengths (Å) and angles (°) for complex **3**

Bond lengths			
Cu1–O2	1.906(6)	Cu4–O4	1.904(6)
Cu1–N1	2.001(7)	Cu4–N7	1.992(7)
Cu1–N2	1.925(7)	Cu4–N8	1.943(7)
Cu1–N3	2.097(8)	Cu4–N9	2.090(7)
Cu1–S1	2.609(3)	Cu4–S3	2.711(3)
Cu2–O1	1.914(6)	Cu5–O3	1.926(6)
Cu2–N4	2.035(8)	Cu5–N10	2.036(7)
Cu2–N5	1.935(7)	Cu5–N11	1.956(7)
Cu2–N6	2.081(8)	Cu5–N12	2.083(7)
Cu2–N13	2.162(8)	Cu5–N14	2.166(8)
Cu3–N15	1.914(12)	Cu3–S2	2.228(4)
Cu3–S3	2.258(3)		
Bond angles			
O2–Cu1–N1	105.3(3)	O4–Cu4–N7	105.5(3)
O2–Cu1–N2	160.2(3)	O4–Cu4–N8	161.5(3)
O2–Cu1–N3	88.7(3)	O4–Cu4–N9	89.4(3)
N1–Cu1–N2	80.0(3)	N7–Cu4–N8	80.1(3)
N1–Cu1–N3	161.7(3)	N7–Cu4–N9	162.7(3)
N2–Cu1–N3	82.9(3)	N8–Cu4–N9	83.1(3)
S1–Cu1–O2	97.9(3)	S3–Cu4–O4	97.5(2)
S1–Cu1–N1	92.85(18)	S3–Cu4–N7	90.46(17)
S1–Cu1–N2	100.9(3)	S3–Cu4–N8	100.1(2)
S1–Cu1–N3	96.9(2)	S3–Cu4–N9	96.3(2)
O1–Cu2–N4	102.7(3)	O3–Cu5–N10	102.4(3)
O1–Cu2–N5	160.3(3)	O3–Cu5–N11	157.9(3)
O1–Cu2–N6	90.6(3)	O3–Cu5–N12	89.6(3)
N4–Cu2–N5	79.8(3)	N10–Cu5–N11	79.9(3)
N4–Cu2–N6	160.8(3)	N10–Cu5–N12	161.6(3)
N5–Cu2–N6	83.1(3)	N11–Cu5–N12	83.7(3)
N13–Cu2–O1	94.6(3)	N14–Cu5–O3	95.6(3)
N13–Cu2–N4	92.8(3)	N14–Cu5–N10	93.4(3)
N13–Cu2–N5	104.9(3)	N14–Cu5–N11	106.3(3)
N13–Cu2–N6	100.0(3)	N14–Cu5–N12	99.3(3)
S2–Cu3–S3	117.84(15)	S2–Cu3–N15	123.4(4)
S3–Cu3–N15	123.4(4)		

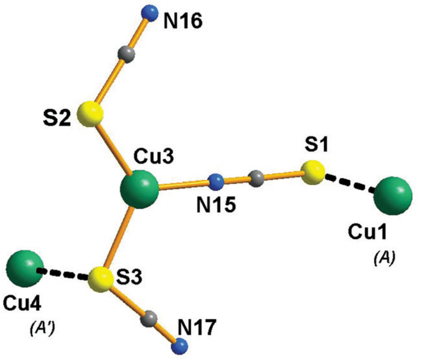

Fig. 6 View of the bridging anionic entity B in complex **3**.

through the Cu^{I}–(SCN)$_3$ bridge giving rise to a pentanuclear cluster.

Infrared spectroscopy

The infrared spectra of complexes **1–3** are in a good agreement with X-ray structural data. These display strong and sharp absorption bands at 1644, 1639 and 1627 cm^{-1}, in **1–3**, respectively, that can be assigned to the >C═N stretching frequency of the coordinated Schiff base ligands HL^1 and HL^2.[35] The coordination of the ligand to the metal center is substantiated by a band appearing at 462, 464 and 469 cm^{-1} for **1–3**, respectively, mainly attributed to the Cu–N stretching,[36] while bands at 1141, 1137 and 1176 cm^{-1} suggest the presence of N–O bonds.[32] Complex **1** exhibits a strong and broad band at *ca.* 3495 cm^{-1}, attributable to ν_s(O–H) vibrations of the coordinated water molecules, and a characteristic double band of the perchlorate anion at 1088–1118 cm^{-1}.[36] The intense doublets at 2130 and 2045 cm^{-1} in the spectra of **2** and **3**, respectively, confirm the presence of the bridging thiocyanate groups.[36]

Variable temperature magnetic susceptibility measurements

The thermal variation of the molar magnetic susceptibility per Cu^{II} dimer times the temperature (χ_mT) show room-temperature values of *ca.* 0.11 and 0.09 emu K mol^{-1} for compounds **1** and **2**, respectively. When the temperature is lowered, χ_mT shows a continuous decrease to reach values close to zero below *ca.* 120 K (Fig. 7). The low room-temperature χ_mT value and its decrease with decreasing temperatures indicate the presence of strong antiferromagnetic interactions in both compounds. This strong antiferromagnetic coupling is also evidenced by the presence of a decrease in the χ_m plot with decreasing temperatures, already observed at room temperature (inset in Fig. 7). The χ_m plot also shows the presence of a Curie-tail at low temperatures, indicative of the presence of a small amount of monomeric paramagnetic impurities due to the presence of Cu^{II} vacancies in some dimers. Since the structure shows the presence of Cu^{II} dimers connected through double Cu–NO–Cu bridges, we have used the classical Bleaney–Bowers $S = 1/2$ dimer model ($H = -2J\hat{S}1\cdot\hat{S}2$) to fit the data.[37] This model reproduces very satisfactorily the magnetic properties of both compounds, with $g = 2.172$, $J = -721$ cm^{-1} and a paramagnetic impurity of 1.5% for compound **1**, and $g = 2.047$, $J = -744$ cm^{-1} and a paramagnetic impurity of 1.2% for compound **2** (solid lines in Fig. 7).

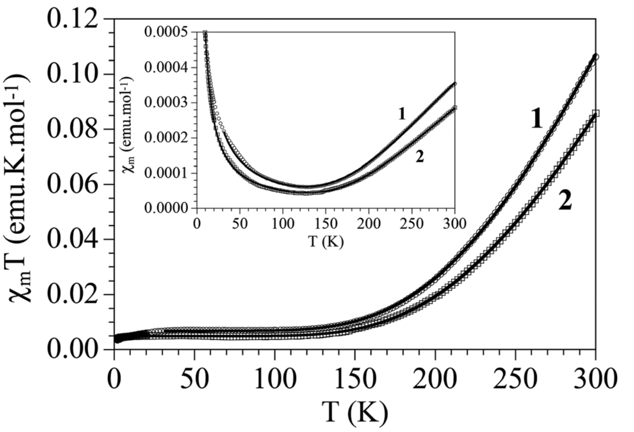

Fig. 7 Thermal variation of χ_mT for compounds **1** (○) and **2** (□). Solid lines represent the best fit to the $S = 1/2$ dinuclear system. Inset shows the thermal variation of χ_m.

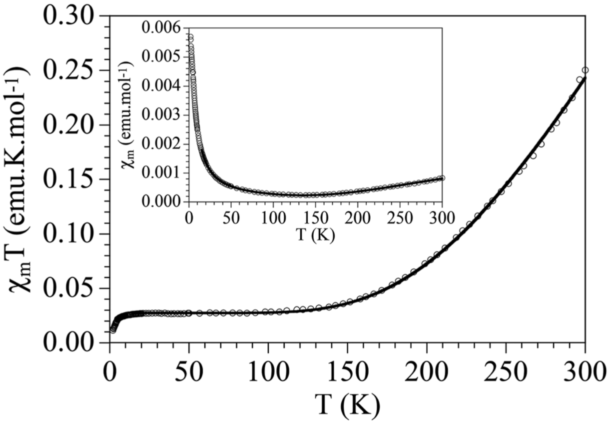

Fig. 8 Thermal variation of $\chi_m T$ for the pentanuclear complex **3**. Solid line represents the best fit to the $S = 1/2$ dinuclear model (see text). Inset shows the thermal variation of χ_m.

As expected, given the structural similarities of the Cu^{II} dimers in compounds **1** and **2**, the obtained *J* values are very similar in both dimers. Note that the similar magnetic behavior in both compounds confirms the assumption that in compound **2** the layer containing Cu2 and Cu3 ions connected through the –NCS– bridges is diamagnetic and, therefore, both copper ions are Cu^{I}.

The thermal variation of the molar magnetic susceptibility per Cu^{II} pentamer (Cu$^{II}_4$Cu^{I}) times the temperature ($\chi_m T$) for compound **3** shows a room-temperature value of *ca.* 0.25 emu K mol^{-1} that decreases continuously as the temperature is lowered to reach a constant value of *ca.* 0.03 emu K mol^{-1} in the temperature range *ca.* 150–10 K. Below 10 K the $\chi_m T$ value shows a more abrupt decrease to reach a value of *ca.* 0.01 emu K mol^{-1} at 2 K (Fig. 8). The room-temperature value is significantly lower than the expected one for four non-interacting $S = 1/2$ Cu^{II} ions (1.5 emu K mol^{-1} if $g = 2$), indicating the presence of a strong antiferromagnetic coupling in the Cu$^{II}_4$Cu^{I} unit. The thermal variation of χ_m confirms this assumption since it shows a soft decrease already at high temperatures, suggesting the presence of a broad maximum above room temperature, as expected for a strong antiferromagnetic coupling.

Although there are five copper ions per formula unit, from the magnetic point of view compound **3** can be considered as formed by two independent Cu(NO)$_2$Cu dimers with two similar double –NO– bridges, separated by a central diamagnetic Cu^{I} ion. Since the structural parameters in both bridges are similar, in a first approach we have assumed that both double μ-NO bridges provide the same coupling constant, *J*, and accordingly, we have reproduced the magnetic moment of compound **3** with a simple Bleaney–Bowers $S = 1/2$ dimer model with only one coupling constant for both dimers.[37] This model reproduces very satisfactorily the magnetic properties of compound **3** with $g = 2.075$, $J = -988$ cm^{-1} and a 1.8% of paramagnetic impurity (solid line in Fig. 8). Since the model with only one coupling constant is already able to reproduce very satisfactorily the magnetic properties of compound **3**, we have not used a more complex model with two different *J* values. Note also that the decrease at very low temperatures cannot be reproduced with this simple model. The inclusion of an interdimer antiferromagnetic coupling with the molecular field approximation model[38] to account for this decrease, does not yield a better fit since the weight of the low temperature data in the fitting procedure is very reduced.

The strong antiferromagnetic couplings observed in compounds **1–3** through the symmetric double –NO– oximato bridge agree very well with all the known examples of similar dimeric Cu^{II} complexes (Table 4). In all these cases, the magnetic coupling through the double –NO– bridges is strong and antiferromagnetic as clearly established by extended-Hückel MO calculations indicating that planar Cu(NO)$_2$Cu rings favor strong antiferromagnetic couplings.[39,40]

From the magnetic data in Table 4 it is clear that all the known examples of symmetric doubly N,O oximato-bridged Cu^{II} dimers present strong antiferromagnetic couplings with *J* values between −446 and *ca.* −1000 cm^{-1}, except in one case where the coupling is smaller (−286 cm^{-1}) due to the presence of significant torsion Cu–N–O–Cu angles and, therefore, to an important lack of planarity in the six-membered Cu(NO)$_2$Cu ring.[41] Although the Cu–O and Cu–N bond distances, as well as the Cu–O–N and Cu–N–O angles may play an important role in determining the final magnetic coupling, the data from Table 4 show that, in most cases, these values are very similar and show no clear tendency, therefore, we cannot establish any reliable magneto-structural correlation based only on these parameters. Since theoretical calculations show that the most important parameter in determining the magnetic coupling must be the planarity of the Cu(NO)$_2$Cu ring,[39,40] we have plotted the magnetic exchange constants of compounds in Table 5 as a function of the average Cu–N–O–Cu dihedral angle (Fig. 9), since this angle reflects the planarity of this ring. Form this plot it is quite evident that there is an approximately linear relationship between the coupling constant and the dihedral Cu–O–N–Cu angle, confirming previous theoretical calculations.[39,40] Interestingly, there are only three points in Fig. 9 (○) that do not follow the linear trend (compounds GUFCIT, HILRID and **3**). In two of these compounds (GUFCIT and **3**), the large average dihedral angles (*ca.* 48.5° and 29.0°) are clearly overestimated since they are in fact due to a large deviation from the average plane of only one oxygen atom (see structures in Table 4). In fact, as also indicated in Table 4, the θ angles (formed between the average plane of the central (NO)$_2$ unit and the two external OCuN units) in both compounds are close to those of other compounds with similar *J* values. In compound HILRID the dihedral Cu–N–O–Cu angle is very small and, accordingly, the coupling should be stronger (*ca.* −900 cm^{-1}). Nevertheless, if we look at the structure (Table 4) we can see that although the central (NO)$_2$ bridges are almost perfectly planar, the Cu ions are far from the average plane of these two central NO bridges (the average distance is larger than 0.5 Å). This large distance is expected to significantly reduce the overlap of the orbitals and, therefore, the magnetic coupling.

Table 4 Magnetic and structural parameters of dimeric Cu^{II} complexes with symmetric double –NO– bridges

CCDC code	J (cm^{-1})	θ^a (°)	d^b (Å)	Cu–O (Å)	Cu–N (Å)	α^c (°)	Ring	Ref.	Structure
BAPVIX	−545	167.79	0.245	1.905	1.989	17.83	Chair	47	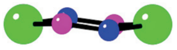
BUQYIW	−720	164.95	0.337	1.914	1.978	23.18	Chair	48	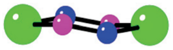
GUFCEP	−825	169.46	0.226	1.901	2.010	15.60	Chair	49	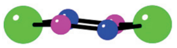
GUFCIT	−550	150.24 155.04	0.610 0.488	1.914 1.949	1.986 1.968	44.20 52.81	Boat Twisted	49	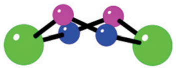
GUFCOZ^d	−510	153.06 163.78	0.312 0.570	1.908 1.919	1.992 1.980	38.64 20.78	Boat Twisted	49	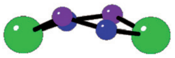
		165.40 153.44	0.249 0.587	1.917 1.916	1.970 1.992	17.36 37.41	Boat Twisted		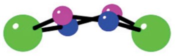
HILRID	−549	155.97 158.28	0.467 0.555	1.915 1.983	1.930 1.936	4.32 0.15	Boat Eclipsed	50	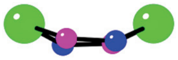
IMIXEI	−504	150.44 150.55	0.567 0.627	1.904 1.936	1.955 1.990	29.59 30.92	Boat Twisted	51	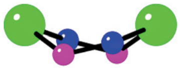
MAXPCU^d	<−1000	169.68	0.212	1.886	2.008	15.65	Chair	52	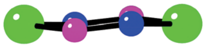
		179.96	0.001	1.887	1.983	0.00	Planar		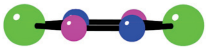
QEVLOS	−722	167.86	0.217	1.936	1.977	19.04	Chair	53	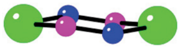
SEGZIO	−286	167.97 169.56	0.118 0.216	1.924 1.905	2.016 1.993	35.86 39.04	Boat Twisted	41	
UMIBIC	−812	179.97	0.001	1.867	2.010	0.04	Planar	54	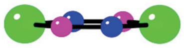
UYEMUH	−718	172.15	0.165	1.906	1.965	12.49	Chair	32	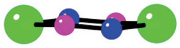
UYENAO^d	−880	156.62 158.80	0.442 0.521	1.929 1.948	1.974 1.977	10.37 14.46	Boat Eclipsed	32	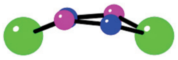
		160.18 157.40	0.520 0.391	1.935 1.929	1.978 1.971	9.01 13.56	Boat Eclipsed		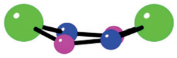
WUFQEU	−800	159.96 156.25	0.445 0.438	1.907 1.904	1.967 1.964	9.38 2.24	Boat Eclipsed	55	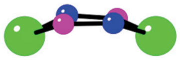
1	−721	159.00 167.88	0.427 0.239	1.882 1.890	2.010 2.004	7.79 19.75	Boat Twisted	This work	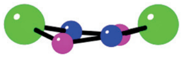
2	−744	166.37	0.275	1.879	1.995	20.25	Chair	This work	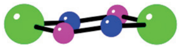
3	−988	167.20 149.29	0.293 0.652	1.906 1.914	2.001 2.035	45.70 14.08	Chair	This work	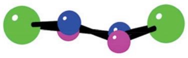
		171.34 151.24	0.150 0.574	1.904 1.926	1.992 2.036	46.09 10.03	Chair		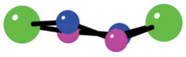

[a] θ = dihedral angle between the planes of each O–Cu–N unit and the average plane of the two NO bridges. [b] d = distance from the Cu^{II} atom(s) to the average plane of the two NO bridges. [c] α = dihedral Cu–N–O–Cu angle. [d] In these compounds there are two different Cu^{II} dimers.

Conclusion

We have synthesized and characterized three novel copper complexes (**1**–**3**) with N_3O donor ketoxime Schiff base ligands presenting similar Cu^{II} dimers connected through double NO bridges. The presence of the same dinuclear Cu^{II} entity in the three complexes shows a tendency of these ligands to form similar dinuclear entities with double NO bridges. The use of NaSCN in **2** and **3** induces the partial reduction of Cu^{II}→Cu^{I} giving rise to a mixed-valence 3D polynuclear network (in **2**) and to a pentanuclear cluster (in **3**). Thus, compound **2** presents 2D anionic layers, of formula $[Cu^{I}_2(SCN)_3]_n^{n-}$, between which the cationic dimers are located. Various bridging modes of SCN$^-$ are observed to be operative in these complexes and, in fact, the Cu^{I}/SCN lattice in **3** is topologically unique. The magnetic coupling observed in the planar Cu^{II}(NO)$_2$Cu^{II} dimers

Table 5 Crystal structure parameters of complexes **1–3**

	1	**2·0.5H$_2$O**	**3**
Empirical formula	$C_{16}H_{36}Cu_2N_6O_{12}Cl_2$	$C_{22}H_{32}Cu_6N_{12}O_{2.5}S_6$	$C_{77}H_{80}Cu_5N_{17}O_4S_5$
Formula weight (g mol^{-1})	702.49	1078.20	1785.65
Wavelength (Å)	0.71073	1.54180	0.71073
Crystal system	Monoclinic	Monoclinic	Monoclinic
Space group	$P2_1/n$ (no. 14)	$P2_1/c$ (no. 14)	$C2/c$ (no. 15)
a (Å)	13.3445(2)	13.655(2)	51.203(4)
b (Å)	12.0554(2)	10.8310(12)	12.5267(7)
c (Å)	17.4604(3)	14.250(1)	29.582(3)
β (°)	90.072(2)	105.53(2)	115.62(1)
V (Å^3)	2808.91(8)	2030.6(4)	17 109(2)
Z	4	2	8
$d_{\text{calc.}}$ (g cm^{-3})	1.661	1.764	1.388
μ (mm^{-1})	1.770	6.646	1.403
F (000)	1448	1076	7344
Crystal size (mm^3)	0.13 × 0.27 × 0.43	0.22 × 0.20 × 0.18	0.06 × 0.10 × 0.49
θ_{range} (°)	3.3–29.2	5.2–58.0	3.0–24.9
Reflections collected	12 528	3968	36 747
Independent collected	6257	2732	11 614
R (int)	0.033	0.0445	0.086
Reflections $I > 2\sigma(I)$	5625	1543	7504
Goodness-of-fit on F^2	1.13	0.95	1.11
final R_1, wR_2 indices	0.0607, 0.0703	0.0445, 0.1227	0.0863, 0.1308
$\Delta\rho_{\max}$, $\Delta\rho_{\min}$ (e Å^{-3})	0.82, −0.92	0.67, −0.24	2.18, −1.00

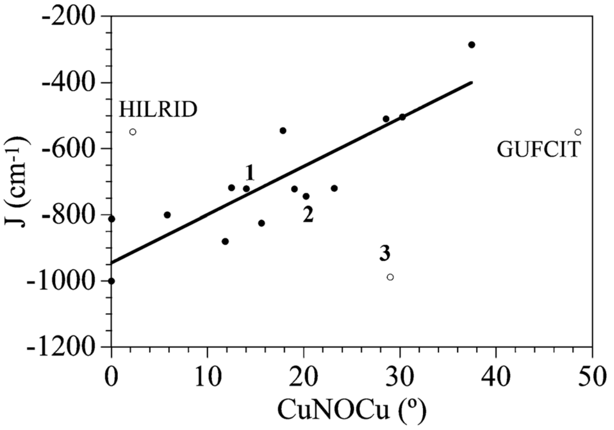

Fig. 9 Relationship between the exchange coupling *J* and the average value of the Cu–N–O–Cu dihedral angle in symmetrical doubly NO-bridged Cu^{II} dimers. The regression line to the filled points (●) is indicated.

is antiferromagnetic and very strong, in agreement with DFT calculation and with magneto-structural correlations in all the structurally and magnetically characterized Cu(NO)$_2$Cu dimers. As expected, the anionic layer (in **2**) and bridge (in **3**) containing Cu^I and SCN$^-$ are diamagnetic.

Experimental section

Materials

All solvents employed for the syntheses were of analytical grade and used as received without further purification. Diacetylmonoxime (Aldrich, Germany), *N*,*N*-dimethylethylenediamine (Fluka), benzilmonoxime, copper acetate, sodium thiocyanate were used as received. Copper perchlorate hexahydrate was prepared by treatment of copper carbonate (E. Merck, India) with 60% perchloric acid (E. Merck, India) followed by slow evaporation on a steam bath. It was then filtered through a fine glass-frit and preserved in a CaCl$_2$ desiccator for further use. All the solvents were of AR grade and used without further purification during synthesis.

Caution! Perchlorate salts are potentially explosive and should be used in small quantity with much care.

Synthesis of Schiff base ligands and copper complexes

Synthesis of [$Me_2N(CH_2)_2N{=}C(CH_3)C(CH_3){=}N(OH)$] (HL^1). The ligand HL^1 was obtained by condensation of diacetylmonoxime (10 mmol, 1.01 g) with *N*,*N*-dimethylethylenediamine (10 mmol, 1.09 mL) in 100 mL of methanol (Scheme 2). On refluxing the methanolic solution for 4 h a pale yellow colored solution was obtained containing the required product that was used without further purification.

Synthesis of [$Me_2N(CH_2)_2N{=}C(C_6H_5)C(C_6H_5){=}N(OH)$] (HL^2). The Schiff base ligand HL^2 was synthesized (Scheme 2) by the condensation of a methanolic solution of benzilmonoxime (10 mmol, 2.25 g) with *N*,*N*-dimethylethylenediamine (10 mmol, 1.09 mL) following the same procedure as for HL^1. The resulting yellow solution of the required product was used without further purification.

Synthesis of [$Cu_2(L^1)_2(H_2O)_2$](ClO_4)$_2$ (1). To a methanolic solution (20 mL) of copper perchlorate hexahydrate (0.370 g, 1 mmol), the methanolic solution of HL^1 (1 mmol, 10 mL) was added with constant stirring for 30 min. The dark green solution was filtered and kept at room temperature for slow evaporation of the solvent. Blue, parallelepiped crystals, suitable for X-ray analysis, were obtained after 14 days. Crystals were filtered and air-dried. Yield: 0.477 g (68%); UV/Vis (acetonitrile): $\lambda_{\max}$ (ε) = 312 (33 695), 417 (3876), 578 nm (560 mol^{-1} dm^3 cm^{-1}); IR (KBr): ν = 1644 (C═N), ν = 3495 (O–H), ν = 1141 (N–O), ν = 1090 (ClO_4), ν = 462 cm^{-1} (Cu–N); elemental analysis calcd (%) for $C_{16}H_{36}Cu_2N_6O_{12}Cl_2$ (702.49): C 27.36, H 5.17, N 11.96; Found: C 27.34, H 5.19, N 11.91.

Synthesis of $\{[Cu^{II}_2(L^1)_2][Cu^{I}_4(\mu_{1,3}\text{-}SCN)_4(\mu_{1,1,3}\text{-}SCN)_2]\}_n$ (2). To a methanolic solution (20 mL) of copper perchlorate hexahydrate (0.370 g, 1 mmol), the methanolic solution of HL^1 (1 mmol, 10 mL) previously prepared (see above) was added followed by dropwise addition of sodium thiocyanate solution (0.080 g, 1 mmol) in the minimum volume of methanol with constant stirring for 20 min. Green, block-shaped crystals, suitable for X-ray analysis, were obtained after 29 days. Crystals were filtered and air-dried. Yield: 0.776 g (72%); UV/Vis (acetonitrile): $\lambda_{\max}$ (ε) = 314 (24 517), 424 (2819), 593 nm (589 mol^{-1} dm^3 cm^{-1}); IR (KBr): ν = 1639 (C═N), ν = 1137 (N–O), ν = 2130 (SCN), ν = 464 cm^{-1} (Cu–N); elemental analysis calcd (%) for $C_{22}H_{32}Cu_6N_{12}O_2S_6$ (1070.23): C 24.69, H 3.01, N 15.71; Found: C 24.64, H 3.03, N 15.69.

Synthesis of $\{[Cu^{II}_2(L^2)_2(NCS)]_2[Cu^{I}(SCN)(\mu_{1,1}\text{-}SCN)(\mu_{1,3}\text{-}SCN)]\}$ (3). This complex was synthesized by using copper acetate (0.199 g, 1 mmol) following a similar procedure as for **2**, but using HL^2 (1 mmol) instead of HL^1. Brown, needle-shaped crystals, suitable for X-ray diffraction, were obtained after 6 days. Crystals were filtered and air-dried. Yield: 0.946 g (53%); UV/Vis (acetonitrile): $\lambda_{\max}$ (ε) = 340 (23 133), 447 (2527), 596 nm (591 mol^{-1} dm^3 cm^{-1}); IR (KBr): ν = 1627 (C═N), ν = 1176 (N–O), ν = 2045 (SCN), ν = 469 cm^{-1} (Cu–N); elemental analysis calcd (%) for $C_{77}H_{80}Cu_5N_{17}O_4S_5$ (1785.63): C 51.79, H 4.52, N 13.34. Found: C 51.77, H 4.53, N 13.35.

Physical measurements

The Fourier transform infrared spectra of the complexes were recorded using a Perkin-Elmer RXI FT-IR spectrophotometer with solid KBr pellets in the range 4000–400 cm^{-1}. The electronic spectra in HPLC-grade acetonitrile were recorded at 300 K using a Perkin-Elmer Lambda 40 (UV-Vis) spectrometer in a 1 cm quartz cuvette in the range 800–200 nm. Elemental analyses (C, H, N) were carried out using a Perkin-Elmer 2400 II elemental analyzer. The magnetic susceptibility measurements were carried out in the temperature range 2–300 K with an applied magnetic field of 0.5 T on polycrystalline samples of compounds **1–3** (with masses of 32.02, 37.55 and 19.18 mg, respectively) with a Quantum Design MPMS-XL-5 SQUID susceptometer. The susceptibility data were corrected for the sample holder previously measured using the same conditions and for the diamagnetic contribution of the salt as deduced by using Pascal's constant tables ($\chi_{\text{dia}} = -335.9 \times 10^{-6}$, -241.6×10^{-6}, and -939.49×10^{-6} emu mol^{-1} for **1**, **2** and **3**, respectively).[42]

X-ray crystallography

X-ray single crystal data collections of **1** and **3** were performed at 293 K using an Oxford Diffraction Gemini diffractometer, equipped with a normal focus, sealed tube X-ray source with graphite monochromated Mo-Kα radiation (λ = 0.71073 Å), using a multi scan technique. Intensities data of **2** were collected on a Cu rotating anode (λ = 1.54178 Å) equipped with a Bruker CCD2000 detector. Data collections and the unit cell refinement of **1** and **3** were performed using CrysAlis RED[43a] software, and for **2** programs Denzo and Scalepack[43b] were employed. All the structures were solved by direct methods using the SIR97[44] program followed by successive difference Fourier syntheses, then refined by full-matrix least squares methods with the programs CRYSTALS[45] (**1** and **2**) and SHELXL-97[46] (**3**). A residual on an inversion center in **2** was interpreted as a disordered water oxygen (occupancy 0.25, H atoms not assigned). All hydrogen atoms were generated geometrically (except those of the water molecules in **1** located on the difference Fourier map) and included in the final cycles of refinement by the riding model approximation. Selected crystallographic data and details of structural refinements are summarized in Table 5.

Acknowledgements

P. Dhal gratefully acknowledges the Council of Scientific and Industrial Research (CSIR), New Delhi, Government of India, for awarding Senior Research Fellowship (SRF) to her [CSIR Sanction No. 09/096(0640)/2010-EMR-I]. We also acknowledge the Spanish MEC (project CTQ2011-26507) and the Generalitat Valenciana (Prometeo 2009/95 and ISIC Programs) for financial support.

References

1 R. Huber, *Angew. Chem.*, 1989, **101**, 849–871.

2 A. Messerschmidt, A. Ressi, R. Ladenstein, R. Huber, M. Bolognesi, G. Gatti, A. Marchesini and A. Finazzi-Agro, *J. Mol. Biol.*, 1989, **206**, 513–529.

3 (*a*) G. A. Ardizzoia, S. Cenini, G. LaMonica, N. Masciocchi and M. Moret, *Inorg. Chem.*, 1994, **33**, 1458–1463; (*b*) G. A. Ardizzoia, M. Angaroni, G. LaMonica, F. Cariati, S. Cenini, M. Moret and N. Masciocchi, *Inorg. Chem.*, 1991, **30**, 4347–4353.

4 *Magnetic Molecular Materials*, ed. D. Gatteschi, O. Kahn, J. S. Miller and F. Palacio, NATO ASI Series 198, Kluwer Academic Publishers, Dordrecht, The Netherlands, 1991.

5 F. H. Jardine, *Adv. Inorg. Chem. Radiochem.*, 1975, **17**, 115–163.

6 B. J. Hathaway, *Struct. Bonding*, 1973, **14**, 49–69.

7 M. Dunaj-Jurčo, G. Ondrejovič and M. Melník, *Coord. Chem. Rev.*, 1988, **83**, 1–28.

8 S. Paul, R. Clćrac, N. G. R. Hearns and D. Ray, *Cryst. Growth Des.*, 2009, **9**, 4032–4040.

9 T. K. Maji, D. Ghoshal, E. Zangrando, J. Ribas and N. R. Chaudhuri, *CrystEngComm*, 2004, **6**, 623–626.

10 (*a*) J.-C. Liu, G.-C. Guo, J.-S. Huang and X.-Z. You, *Inorg. Chem.*, 2003, **42**, 235–243; (*b*) M. S. El. Fallah, F. Badyine, R. Vicente, A. Escuer, X. Solans and M. Font-Bardia, *Chem. Commun.*, 2006, 3113–3115.

11 (*a*) S. Feng, H. Lv, Z. Li, G. Feng, L. Lu and M. Zhu, *CrystEngComm*, 2012, **14**, 98–102; (*b*) T. J. Mooibroek, G. Aromí, M. Quesada, O. Roubeau, P. Gamez, S. D. George, J. v. Slageren, S. Yasin, E. Ruiz and J. Reedijk, *Inorg. Chem.*, 2009, **48**, 10643–10651.

12 (*a*) D. Sadhukhan, C. Rizzoli, E. Garribba, C. J. Gómez-García, A. Yahia-Ammar, L. J. Charbonnièree and S. Mitra, *Dalton Trans.*, 2012, **41**, 11565–11568; (*b*) J. He, J.-X. Zhang, C.-K. Tsang, Z. Xu, Y.-G. Yin, D. Li and S.-W. Ng, *Inorg. Chem.*, 2008, **18**, 7948–7950; (*c*) S. Benmansour, F. Setifi, S. Triki, F. Thétiot, J. Sala-Pala, C. J. Gómez-García and E. Colacio, *Inorg. Chim. Acta*, 2009, **28**, 1308–1314.

13 (*a*) M. Monfort, J. Ribas and X. Solans, *Inorg. Chem.*, 1994, **33**, 4271–4276; (*b*) P. Orioli, B. Bruni, M. D. Vaira, L. Messori and F. Piccioli, *Inorg. Chem.*, 2002, **41**, 4312–4314; (*c*) H. D. Bian, W. Gu, J.-Y. Xu, F. Bian, S.-P. Yan, D.-Z. Liao, Z.-H. Jiang and P. Cheng, *Inorg. Chem.*, 2003, **42**, 4265–4267; (*d*) S. Jana, P. Bhowmik, M. Das, P. P. Jana, K. Harms and S. Chattopadhyay, *Polyhedron*, 2012, **37**, 21–26; (*e*) S. Chattopadhyay, M. G. B. Drew, C. Diaz and A. Ghosh, *Dalton Trans.*, 2007, 2492–2494; (*f*) P. Bhowmik, S. Chattopadhyay, M. G. B. Drew, C. Diaz and A. Ghosh, *Polyhedron*, 2010, **29**, 2637–2642.

14 (*a*) H.-Y. Bie, J.-H. Yu, J.-Q. Xu, J. Lu, Y. Li, X.-B. Cui, X. Zhang, Y.-H. Sun and L.-Y. Pan, *J. Mol. Struct.*, 2003, **660**, 107–112; (*b*) S. Sen, S. Mitra, D. L. Hughes, G. Rosair and C. Desplanches, *Polyhedron*, 2007, **26**, 1740–1744.

15 J. L. Mesa, T. Rojo, M. I. Arriortua, G. Villeneuve, J. V. Folgado, A. Beltran-Porter and D. Beltran-Porter, *J. Chem. Soc., Dalton Trans.*, 1989, 53–56.

16 L. Hou, D. Li, W.-J. Shi, Y.-G. Yin and S. W. Ng, *Inorg. Chem.*, 2005, **44**, 7825–7832.

17 M. A. S. Goher, Q.-C. Yang and T. C. W. Mak, *Polyhedron*, 2000, **19**, 615–621.

18 H. Krautscheid, N. Emig, N. Klaassen and P. Seringer, *J. Chem. Soc., Dalton Trans.*, 1998, 3071–3078.

19 P. Chaudhuri, *Coord. Chem. Rev.*, 2003, **243**, 143–190.

20 A. Chakravorty, *Coord. Chem. Rev.*, 1974, **13**, 1–46.

21 P. K. Nanda, M. Bera, A. M. da C. Ferreira, A. Paduan-Filho and D. Ray, *Polyhedron*, 2009, **28**, 4065–4071.

22 N. F. Curtis, O. P. Gladkikh, S. L. Heath and K. R. Morgan, *Aust. J. Chem.*, 2000, **53**, 577–582.

23 R. Ruiz, J. Sanz, F. Lloret, M. Julve, J. Faus, C. Bois and M. C. Munoz, *J. Chem. Soc., Dalton Trans.*, 1993, 3035–3039.

24 V. V. Pavlishchuk, S. V. Kolotilov, A. W. Addison, M. J. Prushan, R. J. Butcher and L. K. Thompson, *Inorg. Chem.*, 1999, **38**, 1759–1766.

25 F. Birkelbach, M. Winter, U. Florke, H. J. Haupt, C. Butzlaff, M. Lengen, E. Bill, A. X. Trautwein, K. Wieghardt and P. Chaudhuri, *Inorg. Chem.*, 1994, **33**, 3990–4001.

26 V. V. Pavlishchuk, S. V. Kolotilov, A. W. Addison, M. J. Prushan, D. Schollmeyer, L. K. Thompson and E. A. Goreshnik, *Angew. Chem., Int. Ed.*, 2001, **40**, 4734–4737.

27 V. V. Pavlishchuk, S. V. Kolotilov, A. W. Addison, M. J. Prushan, D. Schollmeyer, L. K. Thompson, T. Weyhermueller and E. A. Goreshnik, *Dalton Trans.*, 2003, 1587–1595.

28 R. Ruiz, M. Julve, J. Faus, F. Lloret, M. C. Munoz, Y. Journaux and C. Bois, *Inorg. Chem.*, 1997, **36**, 3434–3439.

29 Y. S. Moroz, K. Kulon, M. Haukka, E. Gumienna-Kontecka, H. Kozłowski, F. Meyer and I. O. Fritsky, *Inorg. Chem.*, 2008, **47**, 5656–5665.

30 B. Cervera, R. Ruiz, F. Lloret, M. Julve, J. Cano, J. Faus, C. Bois and J. Mrozinski, *J. Chem. Soc., Dalton Trans.*, 1997, 395–401.

31 O. Das, N. N. Adarsh, A. Paul and T. K. Paine, *Inorg. Chem.*, 2010, **49**, 541–551.

32 J. P. Naskar, C. Biswas, B. Guhathakurta, N. Aliaga-Alcalde, L. Lu and M. Zhu, *Polyhedron*, 2011, **30**, 2310–2319.

33 A. W. Addison, T. N. Rao, J. Reedijk, J. van. Rijn and G. C. Verschoor, *J. Chem. Soc., Dalton Trans.*, 1984, 1349–1356.

34 J. P. Naskar, B. Guhathakurta, L. Lu and M. Zhu, *Polyhedron*, 2012, **43**, 89–96.

35 K. Nakamoto, *Infrared and Raman Spectra of Inorganic and Coordination Compounds*, Wiley, New York, 5th edn, 1997.

36 M. Maiti, D. Sadhukhan, S. Thakurta, S. Sen, E. Zangrando, R. J. Butcher, R. C. Deka and S. Mitra, *Eur. J. Inorg. Chem.*, 2013, 527–536.

37 B. Bleaney and K. D. Bowers, *Proc. Ro. Soc. London, Ser. A*, 1952, **214**, 451–465.

38 C. J. O'Connor, *Prog. Inorg. Chem.*, 1982, **29**, 203–283.

39 J. M. Dominguez-Vera, E. Colacio, A. Escuer, M. Klinga, R. Kivekäs and A. Romerosa, *Polyhedron*, 1997, **16**, 281–289.

40 R. Ruiz, F. Lloret, M. Julve, M. Carmen Muñoz and C. Bois, *Inorg. Chim. Acta*, 1994, **219**, 179–186.

41 M. Bera, G. Aromi, W. T. Wong and D. Ray, *Chem. Commun.*, 2006, 671–673.

42 G. A. Bain and J. F. Berry, *J. Chem. Educ.*, 2008, **85**, 532–536.

43 (*a*) *Oxford Diffraction, CrysAlis RED*, Oxford Diffraction Ltd, Abingdon, England, 2006; (*b*) Z. Otwinowski and W. Minor, in *Processing of X-ray Diffraction Data Collected in Oscillation Mode, Methods in Enzymology*, vol. 276: *Macromolecular Crystallography*, part A, ed. C. W. Carter Jr. and R. M. Sweet, Academic Press, New York, 1997, pp. 307–326.

44 A. Altomare, M. C. Burla, M. Camalli, G. L. Cascarano, C. Giacovazzo, A. Guagliardi, A. G. G. Moliterni, G. Polidori and R. Spagna, *J. Appl. Crystallogr.*, 1999, **32**, 113–115.

45 D. J. Watkin, C. K. Prout, J. R. Carruthers and P. W. Betteridge, *CRYSTALS*, Issue 11, Chemical Crystallography Laboratory, Oxford, U.K., 1999.

46 G. M. Sheldrick, *Acta Crystallogr., Sect. A: Fundam. Crystallogr.*, 2008, **64**, 112–122.

47 M. Nasakkala, H. Saarinen, J. Korvenranta and E. Nasakkala, *Acta Chem., Scand. Ser. A*, 1981, **35**, 569–574.

48 E. S. Koumousi, C. P. Raptopoulou, S. P. Perlepes, A. Escuer and T. C. Stamatatos, *Polyhedron*, 2010, **29**, 204–211.

49 M. Maekawa, S. Kitagawa, Y. Nakao, S. Sakamoto, A. Yatani, W. Mori, S. Kashino and M. Munakata, *Inorg. Chim. Acta*, 1999, **293**, 20–29.

50 L. K. Thompson, Z. Xu, A. E. Goeta, J. A. K. Howard, H. J. Clase and D. O. Miller, *Inorg. Chem.*, 1998, **37**, 3217–3229.

51 A. Escuer, B. Cordero, M. Font-Bardia and T. Calvet, *Inorg. Chem.*, 2010, **49**, 9752–9754.

52 R. J. Butcher, C. J. O'Connor and E. Sinn, *Inorg. Chem.*, 1979, **18**, 1913–1918.

53 Y. Song, X. Chen, C. Zheng, D. Zhu, X. You and L. Weng, *Transition Met. Chem.*, 2001, **26**, 247–251.

54 A. Escuer, G. Vlahopoulou, S. P. Perlepes, M. Font-Bardia and T. Calvet, *Dalton Trans.*, 2011, **40**, 225–233.

55 V. Mathrubootham, A. W. Addison, K. T. Holman, E. Sinn and L. K. Thompson, *Dalton Trans.*, 2009, 8111–8116.